

Dynamic finite element analysis of nonlocal bars

S Adhikari

College of Engineering, Swansea University, Swansea UK
Email: S.Adhikari@swansea.ac.uk

National University of Defence Technology (NUDT), Changsha, China
April 17, 2014

1 Introduction

2 Axial vibration of damped nonlocal rods

- Equation of motion
- Analysis of damped natural frequencies
- Asymptotic analysis of natural frequencies

3 Dynamic finite element matrix

- Classical finite element of nonlocal rods
- Dynamic finite element for damped nonlocal rod

4 Numerical results and discussions

5 Main Conclusions

- One popularly used size-dependant theory is the nonlocal elasticity theory pioneered by Eringen [1], and has been applied to nanotechnology.
- Nonlocal continuum mechanics is being increasingly used for efficient analysis of nanostructures viz. nanorods [2, 3], nanobeams [4], nanoplates [5, 6], nanorings [7], carbon nanotubes [8, 9], graphenes [10, 11], nanoswitches [12] and microtubules [13]. Nonlocal elasticity accounts for the small-scale effects at the atomistic level.
- In the nonlocal elasticity theory the small-scale effects are captured by assuming that the stress at a point as a function of the strains at all points in the domain:

$$\sigma_{ij}(x) = \int_V \phi(|x - x'|, \alpha) t_{ij} dV(x')$$

where $\phi(|x - x'|, \alpha) = (2\pi\ell^2\alpha^2)K_0(\sqrt{x \bullet x}/\ell\alpha)$

- Nonlocal theory considers long-range inter-atomic interactions and yields results dependent on the size of a body.
- Some of the drawbacks of the classical continuum theory could be efficiently avoided and size-dependent phenomena can be explained by the nonlocal elasticity theory.

- Only limited work on nonlocal elasticity has been devoted to the axial vibration of nanorods.
- Aydogdu [2] developed a nonlocal elastic rod model and applied it to investigate the small scale effect on the axial vibration of clamped-clamped and clamped-free nanorods.
- Filiz and Aydogdu [14] applied the axial vibration of nonlocal rod theory to carbon nanotube heterojunction systems.
- Narendra and Gopalkrishnan [15] have studied the wave propagation of nonlocal nanorods.
- Murmu and Adhikari [16] have studied the axial vibration analysis of a double-nanorod-system. Here, we will be referring to a nanorod as a nonlocal rod, so as to distinguish it from a local rod.

- Several computational techniques have been used for solving the nonlocal governing differential equations. These techniques include Naviers Method [17], Differential Quadrature Method (DQM) [18] and the Galerkin technique [19].
- Recently attempts have been made to develop a Finite Element Method (FEM) based on nonlocal elasticity. The upgraded finite element method in contrast to other methods above can effectively handle more complex geometry, material properties as well as boundary and/or loading conditions.
- Pisano et al. [20] reported a finite element procedure for nonlocal integral elasticity. Recently some motivating work on a finite element approach based on nonlocal elasticity was reported [21].
- The majority of the reported works consider free vibration studies where the effect of non-locality on the eigensolutions has been studied. However, forced vibration response analysis of nonlocal systems has received very little attention.

- Based on the above discussion, in this paper we develop the dynamic finite element method based on nonlocal elasticity with the aim of considering dynamic response analysis.
- The dynamic finite element method belongs to the general class of spectral methods for linear dynamical systems [22].
- This approach, or approaches very similar to this, is known by various names such as the dynamic stiffness method [23–33], spectral finite element method [22, 34] and dynamic finite element method [35, 36].

Dynamic stiffness method

- The mass distribution of the element is treated in an exact manner in deriving the element dynamic stiffness matrix.
- The dynamic stiffness matrix of one-dimensional structural elements, taking into account the effects of flexure, torsion, axial and shear deformation, and damping, is exactly determinable, which, in turn, enables the exact vibration analysis by an inversion of the global dynamic stiffness matrix.
- The method does not employ eigenfunction expansions and, consequently, a major step of the traditional finite element analysis, namely, the determination of natural frequencies and mode shapes, is eliminated which automatically avoids the errors due to series truncation.
- Since modal expansion is not employed, ad hoc assumptions concerning the damping matrix being proportional to the mass and/or stiffness are not necessary.
- The method is essentially a frequency-domain approach suitable for steady state harmonic or stationary random excitation problems.
- The static stiffness matrix and the consistent mass matrix appear as the first two terms in the Taylor expansion of the dynamic stiffness matrix in the frequency parameter.

- So far the dynamic finite element method has been applied to classical local systems only. Now we generalise this approach to nonlocal systems.
- One of the novel features of this analysis is the employment of frequency-dependent complex nonlocal shape functions for damped systems. This in turn enables us to obtain the element stiffness matrix using the usual weak form of the finite element method.
- First we introduce the equation of motion of axial vibration of undamped and damped rods.
- Natural frequencies and their asymptotic behaviours for both cases are discussed for different boundary conditions.
- The conventional and the dynamic finite element method are developed. Closed form expressions are derived for the mass and stiffness matrices.
- The proposed methodology is applied to an armchair single walled carbon nanotube (SWCNT) for illustration. Theoretical results, including the asymptotic behaviours of the natural frequencies, are numerically illustrated.

Equation of motion

The equation of motion of axial vibration for a damped nonlocal rod can be expressed as

$$EA \frac{\partial^2 U(x, t)}{\partial x^2} + \hat{c}_1 \left(1 - (e_0 a)_1^2 \frac{\partial^2}{\partial x^2} \right) \frac{\partial^3 U(x, t)}{\partial x^2 \partial t} \\ = \hat{c}_2 \left(1 - (e_0 a)_2^2 \frac{\partial^2}{\partial x^2} \right) \frac{\partial U(x, t)}{\partial t} + \left(1 - (e_0 a)^2 \frac{\partial^2}{\partial x^2} \right) \left\{ m \frac{\partial^2 U(x, t)}{\partial t^2} + F(x, t) \right\} \quad (1)$$

- This is an extension of the equation of motion of an undamped nonlocal rod for axial vibration [2, 16, 37].
- Here EA is the axial rigidity, m is mass per unit length, $e_0 a$ is the nonlocal parameter [1], $U(x, t)$ is the axial displacement, $F(x, t)$ is the applied force, x is the spatial variable and t is the time.
- The constant \hat{c}_1 is the strain-rate-dependent viscous damping coefficient and \hat{c}_2 is the velocity-dependent viscous damping coefficient. The parameters $(e_0 a)_1$ and $(e_0 a)_2$ are nonlocal parameters related to the two damping terms respectively. For simplicity we have not taken into account any nonlocal effect related to the damping. In the following analysis we consider $(e_0 a)_1 = (e_0 a)_2 = 0$.

- Assuming harmonic response as

$$U(x, t) = u(x) \exp [i\omega t] \quad (2)$$

and considering free vibration, from Eq. (1) we have

$$\left(1 + i\omega \frac{\hat{c}_1}{EA} - \frac{m\omega^2}{EA} (e_0 a)^2 \right) \frac{d^2 u}{dx^2} + \left(\frac{m\omega^2}{EA} - i\omega \frac{\hat{c}_2}{EA} \right) u(x) = 0 \quad (3)$$

- Following the damping convention in dynamic analysis [38], we consider stiffness and mass proportional damping. Therefore, we express the damping constants as

$$\hat{c}_1 = \zeta_1 (EA) \quad \text{and} \quad \hat{c}_2 = \zeta_2 (m) \quad (4)$$

where ζ_1 and ζ_2 are stiffness and mass proportional damping factors. Substituting these, from Eq. (3) we have

$$\frac{d^2 u}{dx^2} + \alpha^2 u = 0 \quad (5)$$

- Here

$$\alpha^2 = \frac{(\omega^2 - i\zeta_2\omega) / c^2}{(1 + i\omega\zeta_1 - (e_0a)^2\omega^2/c^2)} \quad (6)$$

with

$$c^2 = \frac{EA}{m} \quad (7)$$

- It can be noticed that α^2 is a complex function of the frequency parameter ω .
- In the special case of undamped systems when damping coefficients ζ_1 and ζ_2 go to zero, α^2 in Eq. (6) reduces to

$$\alpha^2 = \frac{\Omega^2}{1 - (e_0a)^2\Omega^2}$$

where $\Omega^2 = \omega^2/c^2$, which is a real function of ω .

- In a further special case of undamped local systems when the nonlocal parameter e_0a goes to zero, α^2 in Eq. (6) reduces to Ω^2 , that is,

$$\alpha^2 = \Omega^2 = \omega^2/c^2$$

Damped natural frequencies

- Natural frequencies of undamped nonlocal rods have been discussed in the literature [2]. Natural frequencies of damped systems receive little attention. The **damped natural frequency** depends on the boundary conditions.
- We denote a parameter σ_k as

$$\sigma_k = \frac{k\pi}{L}, \quad \text{for clamped-clamped boundary conditions} \quad (8)$$

$$\text{and } \sigma_k = \frac{(2k-1)\pi}{2L}, \quad \text{for clamped-free boundary conditions} \quad (9)$$

- Following the **conventional approach** [38], the natural frequencies can be obtained from

$$\alpha = \sigma_k \quad (10)$$

- Taking the square of this equation and denoting the natural frequencies as ω_k we have

$$(\omega_k^2 - i\zeta_2\omega_k) = \sigma_k^2 c^2 (1 + i\omega_k\zeta_1 - (\mathbf{e}_0 \mathbf{a})^2 \omega_k^2 / c^2) \quad (11)$$

- Rearranging we obtain

$$\omega_k^2 (1 + \sigma_k^2 (\mathbf{e}_0 \mathbf{a})^2) - i\omega_k (\zeta_2 + \zeta_1 \sigma_k^2 c^2) - \sigma_k^2 c^2 = 0 \quad (12)$$

This is a very generic equation and many special cases can be obtained from this as follows:

- *Undamped local systems*: This case can be obtained by substituting $\zeta_1 = \zeta_2 = 0$ and $e_0 a = 0$. From Eq. (12) we therefore obtain

$$\omega_k = \sigma_k C \quad (13)$$

which is the classical expression [38].

- *Undamped nonlocal systems*: This case can be obtained by substituting $\zeta_1 = \zeta_2 = 0$. Solving Eq. (12) we therefore obtain

$$\omega_k = \frac{\sigma_k C}{\sqrt{1 + \sigma_k^2 (e_0 a)^2}} \quad (14)$$

which is obtained in [2].

- *Damped local systems*: This case can be obtained by substituting $\zeta_1 = \zeta_2 = 0$. Solving Eq. (12) we obtain

$$\omega_k = i (\zeta_2 + \zeta_1 \sigma_k^2 c^2) / 2 \pm \sigma_k c \sqrt{1 - (\zeta_1 \sigma_k c + \zeta_2 / (\sigma_k c))^2 / 4} \quad (15)$$

Therefore, the decay rate is $(\zeta_2 + \zeta_1 \sigma_k^2 c^2) / 2$ and damped oscillation frequency is $\sigma_k c \sqrt{1 - (\zeta_1 \sigma_k c + \zeta_2 / (\sigma_k c))^2 / 4}$. We observe that damping effectively reduces the oscillation frequency.

Damped natural frequencies

- For the general case of a nonlocal damped system, the damped frequency can be obtained by solving Eq. (12) as

$$\omega_k = \frac{i(\zeta_2 + \zeta_1 \sigma_k^2 c^2)}{2(1 + \sigma_k^2 (e_0 a)^2)} \pm \frac{\sigma_k c}{\sqrt{1 + \sigma_k^2 (e_0 a)^2}} \sqrt{1 - \frac{(\zeta_1 \sigma_k c + \zeta_2 / (\sigma_k c))^2}{4(1 + \sigma_k^2 (e_0 a)^2)}} \quad (16)$$

- Therefore, the decay rate is given by $\frac{(\zeta_2 + \zeta_1 \sigma_k^2 c^2)}{2(1 + \sigma_k^2 (e_0 a)^2)}$ and the damped oscillation frequency is given by

$$\omega_{d_k} = \frac{\sigma_k c}{\sqrt{1 + \sigma_k^2 (e_0 a)^2}} \sqrt{1 - \frac{(\zeta_1 \sigma_k c + \zeta_2 / (\sigma_k c))^2}{4(1 + \sigma_k^2 (e_0 a)^2)}} \quad (17)$$

It can be observed that the nonlocal damped system has the lowest natural frequencies. Note that the expressions derived here are general in terms of the boundary conditions.

Asymptotic natural frequencies

- We are interested in dynamic response analysis of damped nonlocal rods. As a result, behaviour of the natural frequencies across a wide frequency range is of interest.
- An asymptotic analysis is conducted here to understand the frequency behaviour in the high frequency limit. We first consider the undamped natural frequency given by Eq. (14).
- To obtain asymptotic values, we rewrite the frequency equation in (14) and take the mathematical limit $k \rightarrow \infty$ to obtain

$$\lim_{k \rightarrow \infty} \omega_k = \lim_{k \rightarrow \infty} \frac{c}{\sqrt{\frac{1}{\sigma_k^2} + (e_0 a)^2}} = \frac{c}{(e_0 a)} = \frac{1}{(e_0 a)} \sqrt{\frac{EA}{m}} \quad (18)$$

- This is obtained by noting the fact that for $k \rightarrow \infty$, for both sets of boundary conditions we have $\sigma_k \rightarrow \infty$. The result in Eq. (18) shows that there exists an 'upper limit' of frequency in nonlocal systems.

- This upper limit of frequency is an inherent property of a nonlocal system. It is a function of material properties only and independent of the boundary conditions and the length of the rod.
- The smaller the value of $e_0 a$, the larger this upper limit becomes. Eventually for a local system $e_0 a = 0$ and the upper limit becomes infinite, which is well known.
- We consider a SWCNT to illustrate the theory. An armchair (5, 5) SWCNT with Young's modulus $E = 6.85$ TPa, $L = 25$ nm, density $\rho = 9.517 \times 10^3$ kg/m³ and thickness $t = 0.08$ nm is considered as in [39].

Axial vibration of a single-walled carbon nanotube

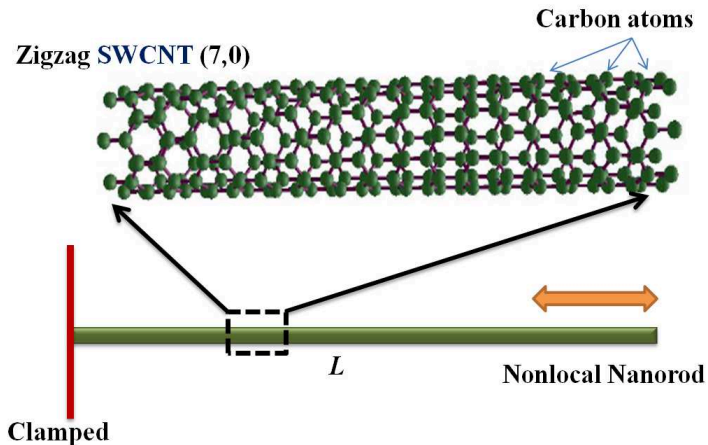
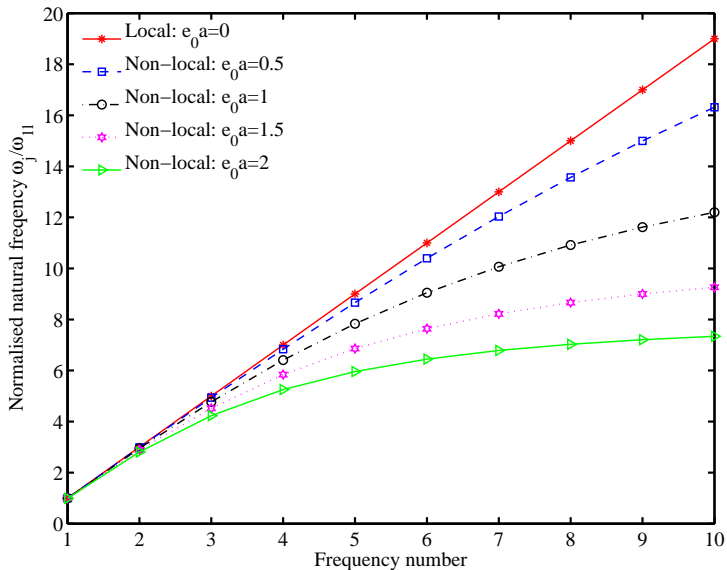


Figure : Axial vibration of a armchair (5, 5) single-walled carbon nanotube (SWCNT) with clamped-free boundary condition.

Nonlocal natural frequencies of SWCNT



First 10 undamped natural frequencies for the axial vibration of SWCNT.

- The frequency plot clearly shows that the natural frequencies decrease with increasing value of the nonlocal parameter $e_0 a$.
- One interesting feature arising for larger values of $e_0 a$ is that the frequency curve effectively becomes 'flat'. This implies that the natural frequencies reach a terminal value as shown by the asymptotic analysis
- Using Eq. (18), for large values of k , the normalised natural frequency plotted in the figure would approach to

$$\frac{\omega_k}{\omega_{11}} \approx \frac{2/\pi}{(e_0 a/L)} \quad (19)$$

- Therefore, for $e_0 a = 2$ nm, we have $\omega_{k_{\max}} \leq 7.957$. Clearly, the smaller the value of $e_0 a$, the larger this upper limit becomes.

Damped asymptotic frequency

- Now we turn our attention to the oscillation frequency of the damped system.
- Rewriting the expressions for the oscillation frequency from Eq. (17) and taking the limit as $k \rightarrow \infty$ we obtain

$$\begin{aligned}\lim_{k \rightarrow \infty} \omega_{d_k} &= \lim_{k \rightarrow \infty} \frac{c}{\sqrt{\frac{1}{\sigma_k^2} + (e_0 a)^2}} \sqrt{1 - \frac{\left(\zeta_1 c + \frac{1}{\sigma_k^2} (\zeta_2 / c)\right)^2}{4 \left(\frac{1}{\sigma_k^2} + (e_0 a)^2\right)}} \\ &= \frac{c}{(e_0 a)} \sqrt{1 - \left(\frac{\zeta_1 c}{2e_0 a}\right)^2} \quad (20)\end{aligned}$$

- Therefore the upper frequency limit for the damped systems is lower than that of the undamped system.
- It is interesting note that it is independent of the mass proportional damping ζ_2 . Only the stiffness proportional damping has an effect on the upper frequency limit.

Asymptotic critical damping factor

- Equation (20) can also be used to obtain an asymptotic critical damping factor. For vibration to continue, the term within the square root in Eq. (20) must be greater than zero.
- Therefore, the asymptotic critical damping factor for nonlocal rods can be obtained with $\lim_{k \rightarrow \infty} \omega_{d_k} = 0$ as

$$(\zeta_1)_{\text{crit}} = \frac{2e_0 a}{c} \quad (21)$$

- In practical terms, this implies that the value of ζ_1 should be less than this value for high frequency vibration.
- Again observe that like the upper frequency limit, the asymptotic critical damping factor is a function of material properties only and independent of the boundary conditions and the length of the rod.
- The asymptotic critical damping factor is independent of ζ_2 .

- The spacing between the natural frequencies is important for dynamic response analysis as the shape of the frequency response function depends on the spacing.
- Because k is an index, the derivative $\frac{d\omega_k}{dk}$ is not meaningful as k is an integer. However, in the limit $k \rightarrow \infty$, we can obtain mathematically $\frac{d\omega_k}{dk}$ and it would mean the rate of change of frequencies with respect to the counting measure. This in turn is directly related to the frequency spacing.
- For the local rod it is well known that frequencies are uniformly spaced. This can be seen by differentiating ω_k in Eq. (13) as

$$\lim_{k \rightarrow \infty} \frac{d\omega_k}{dk} = c \frac{d\sigma_k}{dk}, \quad \text{where} \quad \frac{d\sigma_k}{dk} = \frac{\pi}{L} \quad (22)$$

for both sets of boundary conditions.

- For nonlocal rods, from Eq. (14) we have

$$\begin{aligned}\lim_{k \rightarrow \infty} \frac{d\omega_k}{dk} &= \lim_{k \rightarrow \infty} \frac{d}{dk} \left(\frac{c}{\sqrt{\frac{1}{\sigma_k^2} + (e_0 a)^2}} \right) = \lim_{k \rightarrow \infty} \frac{\pi}{L} \frac{c}{\left(\frac{1}{\sigma_k^2} + (e_0 a)^2\right)^{3/2} \sigma_k^2} \\ &= \lim_{k \rightarrow \infty} \frac{\pi}{L} \frac{c}{(e_0 a)^3} \frac{1}{\sigma_k^2} = 0\end{aligned}\tag{23}$$

- The limit in the preceding equation goes to zero because $\sigma_k \rightarrow \infty$ for $k \rightarrow \infty$.
- This shows that unlike local systems, for large values of k , the undamped natural frequencies of nonlocal rods will tend to cluster together.
- A similar conclusion can be drawn by considering the damped natural frequencies also.

- We consider an element of length ℓ_e with axial stiffness EA and mass per unit length m .



Figure : A nonlocal element for the axially vibrating rod with two nodes. It has two degrees of freedom and the displacement field within the element is expressed by linear shape functions.

- This element has two degrees of freedom and there are two shape functions $N_1(x)$ and $N_2(x)$. The shape function matrix for the axial deformation [40] can be given by

$$\mathbf{N}(x) = [N_1(x), N_2(x)]^T = [1 - x/L, x/L]^T \quad (24)$$

- Using this the stiffness matrix can be obtained using the conventional variational formulation as

$$\mathbf{K}_e = EA \int_0^L \frac{d\mathbf{N}(x)}{dx} \frac{d\mathbf{N}^T(x)}{dx} dx = \frac{EA}{L} \begin{bmatrix} 1 & -1 \\ -1 & 1 \end{bmatrix} \quad (25)$$

- The mass matrix for the nonlocal element can be obtained as

$$\begin{aligned} \mathbf{M}_e &= m \int_0^L \mathbf{N}(x) \mathbf{N}^T(x) dx + m(e_0 a)^2 \int_0^L \frac{d\mathbf{N}(x)}{dx} \frac{d\mathbf{N}^T(x)}{dx} dx \\ &= \frac{mL}{6} \begin{bmatrix} 2 & 1 \\ 1 & 2 \end{bmatrix} + mL(e_0 a/L)^2 \begin{bmatrix} 1 & -1 \\ -1 & 1 \end{bmatrix} \\ &= mL \begin{bmatrix} 1/3 + (e_0 a/L)^2 & 1/6 - (e_0 a/L)^2 \\ 1/6 - (e_0 a/L)^2 & 1/3 + (e_0 a/L)^2 \end{bmatrix} \end{aligned} \quad (26)$$

- For the special case when the rod is local, the mass matrix derived above reduces to the classical mass matrix [40, 41] as $e_0 a = 0$.

- The first step for the derivation of the dynamic element matrix is the generation of dynamic shape functions.
- The dynamic shape functions are obtained such that the equation of dynamic equilibrium is satisfied exactly at all points within the element.
- Similarly to the classical finite element method, assume that the frequency-dependent displacement within an element is interpolated from the nodal displacements as

$$u_e(x, \omega) = \mathbf{N}^T(x, \omega) \hat{\mathbf{u}}_e(\omega) \quad (27)$$

- Here $\hat{\mathbf{u}}_e(\omega) \in \mathbb{C}^n$ is the nodal displacement vector $\mathbf{N}(x, \omega) \in \mathbb{C}^n$ is the vector of frequency-dependent shape functions and $n = 2$ is the number of the nodal degrees-of-freedom.

- Suppose the $s_j(x, \omega) \in \mathbb{C}, j = 1, 2$ are the basis functions which exactly satisfy Eq. (5).
- It can be shown that the shape function vector can be expressed as

$$\mathbf{N}(x, \omega) = \mathbf{\Gamma}(\omega)\mathbf{s}(x, \omega) \quad (28)$$

where the vector $\mathbf{s}(x, \omega) = \{s_j(x, \omega)\}^T, \forall j = 1, 2$ and the complex matrix $\mathbf{\Gamma}(\omega) \in \mathbb{C}^{2 \times 2}$ depends on the boundary conditions.

- In order to obtain $\mathbf{s}(x, \omega)$ first assume that

$$u(x) = \bar{u} \exp[kx] \quad (29)$$

where k is the wave number. Substituting this in Eq. (5) we have

$$k^2 + \alpha^2 = 0 \quad \text{or} \quad k = \pm i\alpha \quad (30)$$

- In view of the solutions in Eq. (30), the complex displacement field within the element can be expressed by a linear combination of the basis functions $e^{-i\alpha x}$ and $e^{i\alpha x}$ so that in our notations $\mathbf{s}(x, \omega) = \{e^{-i\alpha x}, e^{i\alpha x}\}^T$.
- Therefore, it is more convenient to express $\mathbf{s}(x, \omega)$ in terms of trigonometric functions. Considering $e^{\pm i\alpha x} = \cos(\alpha x) \pm i \sin(\alpha x)$, the vector $\mathbf{s}(x, \omega)$ can be alternatively expressed as

$$\mathbf{s}(x, \omega) = \begin{Bmatrix} \sin(\alpha x) \\ \cos(\alpha x) \end{Bmatrix} \in \mathbb{C}^2 \quad (31)$$

- Considering unit axial displacement boundary condition as $u_e(x=0, \omega) = 1$ and $u_e(x=L, \omega) = 1$, after some elementary algebra, the shape function vector can be expressed in the form of Eq. (28) as

$$\mathbf{N}(x, \omega) = \mathbf{\Gamma}(\omega) \mathbf{s}(x, \omega), \quad \text{where} \quad \mathbf{\Gamma}(\omega) = \begin{bmatrix} -\cot(\alpha L) & 1 \\ \operatorname{cosec}(\alpha L) & 0 \end{bmatrix} \in \mathbb{C}^{2 \times 2} \quad (32)$$

- Simplifying this we obtain the dynamic shape functions as

$$\mathbf{N}(x, \omega) = \begin{bmatrix} -\cot(\alpha L) \sin(\alpha x) + \cos(\alpha x) \\ \operatorname{cosec}(\alpha L) \sin(\alpha x) \end{bmatrix} \quad (33)$$

- Taking the limit as ω goes to 0 (that is the static case) it can be shown that the shape function matrix in Eq. (33) reduces to the classical shape function matrix given by Eq. (24). Therefore the shape functions given by Eq. (33) can be viewed as the generalisation of the nonlocal dynamical case.

Dynamic stiffness matrix

- The stiffness and mass matrices can be obtained similarly to the static finite element case discussed before.
- Note that for this case all the matrices become complex and frequency-dependent.
- It is more convenient to define the dynamic stiffness matrix as

$$\mathbf{D}_e(\omega) = \mathbf{K}_e(\omega) - \omega^2 \mathbf{M}_e(\omega) \quad (34)$$

so that the equation of dynamic equilibrium is

$$\mathbf{D}_e(\omega) \hat{\mathbf{u}}_e(\omega) = \hat{\mathbf{f}}(\omega) \quad (35)$$

- In Eq. (34), the frequency-dependent stiffness and mass matrices can be obtained as

$$\mathbf{K}_e(\omega) = EA \int_0^L \frac{d\mathbf{N}(x, \omega)}{dx} \frac{d\mathbf{N}^T(x, \omega)}{dx} dx$$

$$\text{and } \mathbf{M}_e(\omega) = m \int_0^L \mathbf{N}(x, \omega) \mathbf{N}^T(x, \omega) dx \quad (36)$$

- After some algebraic simplifications [31, 42] it can be shown that the dynamic stiffness matrix is given by the following closed-form expression

$$\mathbf{D}_e(\omega) = EA\alpha \begin{bmatrix} \cot(\alpha L) & -\operatorname{cosec}(\alpha L) \\ \operatorname{cosec}(\alpha L) & \cot(\alpha L) \end{bmatrix} \quad (37)$$

- This is in general a 2×2 matrix with complex entries. The frequency response of the system at the nodal point can be obtained by simply solving Eq. (35) for all frequency values.
- The calculation only involves inverting a 2×2 complex matrix and the results are exact with only one element for any frequency value.
- This is a significant advantage of the proposed dynamic finite element approach compared to the conventional finite element approach discussed in the previous subsection.

- A distributed body force can be considered following the usual finite element approach [40] and replacing the static shape functions with the dynamic shape functions (33).
- Suppose $p_e(x, \omega)$, $x \in [0, L]$ is the frequency depended distributed body force. The element nodal forcing vector can be obtained as

$$\mathbf{f}_e(\omega) = \int_0^L p_e(x, \omega) \mathbf{N}(x, \omega) dx \quad (38)$$

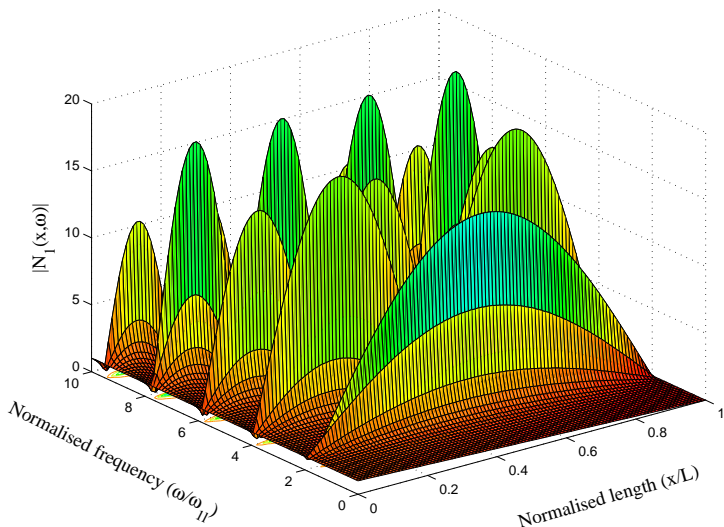
- As an example, if a point harmonic force of magnitude p is applied at length $b < L$ then, $p_e(x, \omega) = p\delta(x - b)$ where $\delta(\bullet)$ is the Dirac delta function.
- The element nodal force vector becomes

$$\mathbf{f}_e(\omega) = p \int_0^L \delta(x - b) \mathbf{N}(x, \omega) dx = p \left\{ \begin{array}{c} -\cot(\alpha L) \sin(\alpha b) + \cos(\alpha b) \\ \operatorname{cosec}(\alpha L) \sin(\alpha b) \end{array} \right\} \quad (39)$$

Numerical example

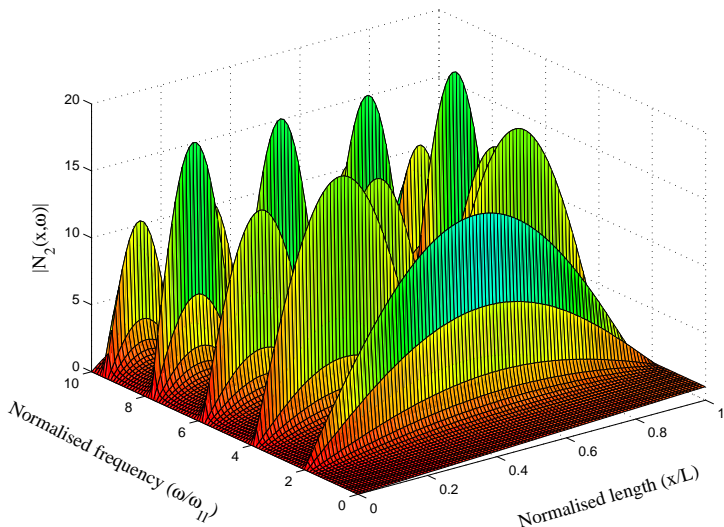
- We consider only mass proportional damping such that the damping factor $\zeta_2 = 0.05$ and $\zeta_1 = 0$.
- A range of values of $e_0 a$ within 0-2 nm are used to understand its role in the dynamic response.
- Although the role of the nonlocal parameter on the natural frequencies has been investigated, its effect on the dynamic response is relatively unknown.
- It is assumed that the SWCNT is fixed at one end and we are interested in the frequency response at the free end due to harmonic excitation.
- Using the dynamic finite element approach only one 'finite element' is necessary as the equation of motion is solved exactly.
- We consider dynamic response of the CNT due to a harmonic force at the free edge.

Shape function $N_1(x, \omega)$ for $e_0 a = 0.5$ nm



Amplitude of the shape function $N_1(x, \omega)$ with normalised frequency axes.

Shape function $N_2(x, \omega)$ for $e_0 a = 0.5$ nm



Amplitude of the shape function $N_2(x, \omega)$ with normalised frequency axes.

- The amplitudes of the two dynamic shape functions as a function of frequency for $e_0 a = 0.5$ nm are shown.
- For convenience, the shape functions are plotted against normalised frequency

$$\hat{\omega} = \omega/\omega_{1l} \quad (40)$$

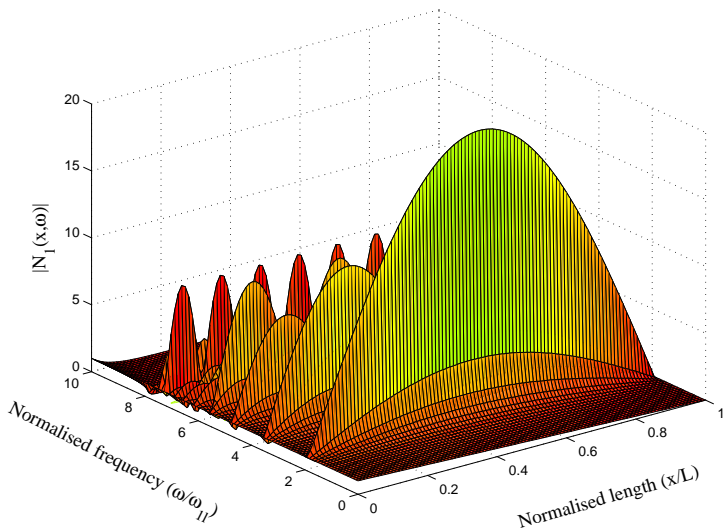
and normalised length coordinate x/L .

- Here ω_{1l} is the first natural frequency of the local rod [38], given by

$$\omega_{1l} = \frac{\pi}{2L} \sqrt{\frac{EA}{m}} \quad (41)$$

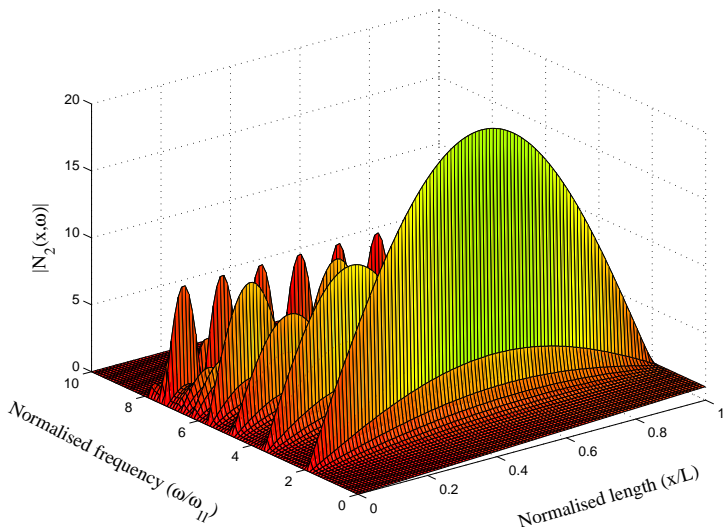
- The amplitudes of the two dynamic shape functions as a function of frequency for $e_0 a = 2.0$ nm are shown next to examine the influence of the nonlocal parameter on the dynamic shape functions.

Shape function $N_1(x, \omega)$ for $e_0 a = 2.0$ nm



Amplitude of the shape function $N_1(x, \omega)$ with normalised frequency axes.

Shape function $N_2(x, \omega)$ for $e_0 a = 2.0$ nm

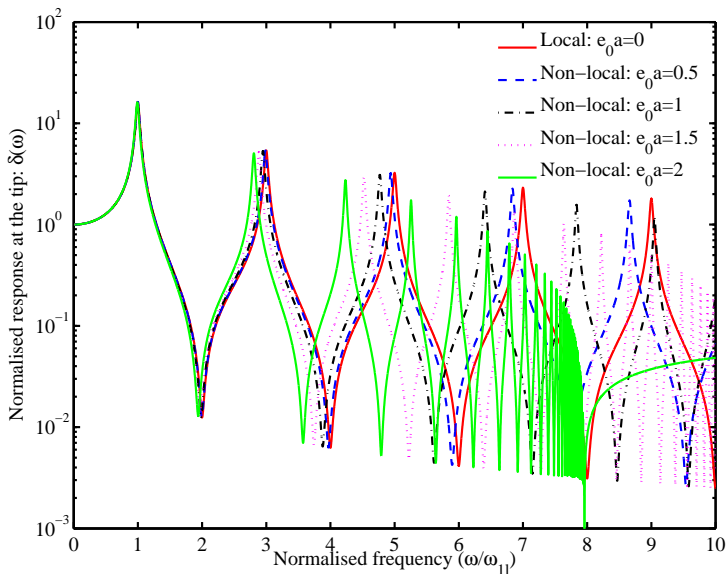


Amplitude of the shape function $N_2(x, \omega)$ with normalised frequency axes.

The plots of the shape functions show the following interesting features:

- 1 At zero frequency (that is for the static case) the shape functions reduce to the classical linear functions given by Eq. (24). It can be observed that $N_1(0, 0) = 1$, $N_2(L, 0) = 0$ and $N_2(0, 0) = 0$, $N_2(L, 0) = 1$.
- 2 For increasing frequency, the shape functions become nonlinear in x and adapt themselves according to the vibration modes. One can observe multiple modes in the higher frequency range. This nonlinearity in the shape functions is the key for obtaining the exact dynamic response using the proposed approach.
- 3 The figures also show the role of the nonlocal parameter. For the case of $e_0 a = 2.0$ nm one can observe more number of modes in the high frequency range. This is due to the fact that natural frequency of the nonlocal rod reduced with the increase in the value of the nonlocal parameter.

Frequency response



Normalised dynamic frequency response amplitude.

- The normalised displacement amplitude is defined by

$$\delta(\omega) = \frac{\hat{u}_2(\omega)}{u_{\text{static}}} \quad (42)$$

where u_{static} is the static response at the free edge given by $u_{\text{static}} = FL/EA$.

- Assuming the amplitude of the harmonic excitation at the free edge is F , the dynamic response can be obtained using the equation of dynamic equilibrium (35) as

$$\hat{u}_2(\omega) = \frac{F}{EA\alpha \cot(\alpha L)} = \frac{F \tan(\alpha L)}{EA\alpha} \quad (43)$$

- Therefore, the normalised displacement amplitude in Eq. (42) is given by

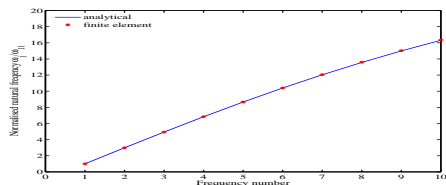
$$\delta(\omega) = \frac{\hat{u}_2(\omega)}{u_{\text{static}}} = \left(\frac{F \tan(\alpha L)}{EA\alpha} \right) / (FL/EA) = \frac{\tan(\alpha L)}{\alpha L} \quad (44)$$

- The frequency axis of the response amplitude is normalised similarly to the plots of the shape functions given earlier.

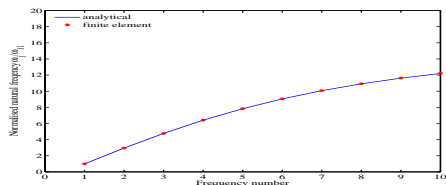
- The consequence of the asymptotic upper limit can be seen in the frequency response amplitude plot.
- For higher values $\epsilon_0 a$, more and more resonance peaks are clustered within a frequency band.
- Indeed in Eq. (23) we have proved that asymptotically, the spacing between the natural frequencies goes to zero. This implies that higher natural frequencies of a nonlocal system are very closely spaced.
- This fact can be observed in the frequency band $7 \lesssim \hat{\omega} \lesssim 8$ for the case when $\epsilon_0 a = 2$ nm. The same behaviour is expected for other values of $\epsilon_0 a$ in the higher frequency ranges.
- It is worth pointing out that the frequency response curve for the case of $\epsilon_0 a = 2.0$ nm is invalid after $\hat{\omega} > 8$ as it is beyond the maximum frequency limit.
- It can also be seen that the resonance peak shifts to the left for increasing values of $\epsilon_0 a$. This shift corresponds to the reduction in the natural frequencies as shown in before.

- We compare the results from the dynamic finite element and conventional finite element methods.
- The natural frequencies can be obtained using the conventional nonlocal finite element method.
- By assembling the element stiffness and mass matrices given by Eqs. (25) and (26) and solving the resulting matrix eigenvalue problem $\mathbf{K}\phi_j = \omega_j^2 \mathbf{M}\phi_j, j = 1, 2, \dots$ one can obtain the both the eigenvalues and eigenvectors (denoted by ϕ_j here).
- For the numerical calculation we used 100 elements. This in turn, results in global mass and stiffness matrices of dimension 200×200 .

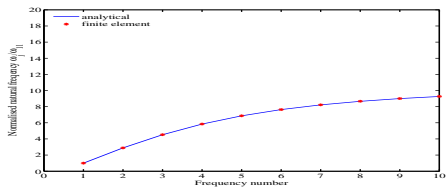
Dynamic vs. conventional FEM



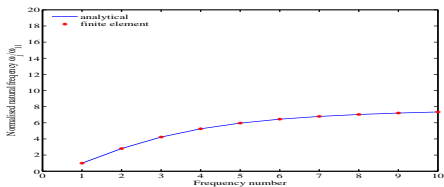
(a) $e_0 a = 0.5 \text{ nm}$



(b) $e_0 a = 1.0 \text{ nm}$



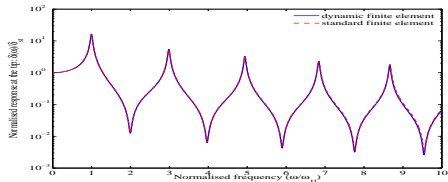
(c) $e_0 a = 1.5 \text{ nm}$



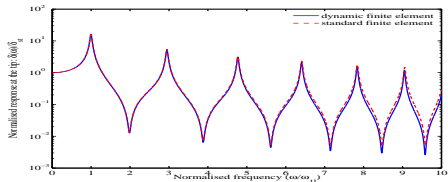
(d) $e_0 a = 2.0 \text{ nm}$

Figure : Normalised natural frequency (ω_j/ω_{11}) at the tip for different values of $e_0 a$. Analytical results are compared with the finite element (with 100 elements) results.

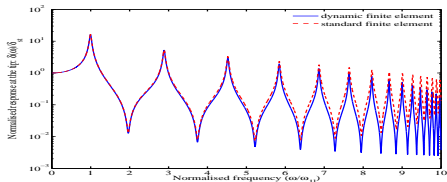
Dynamic vs. conventional FEM



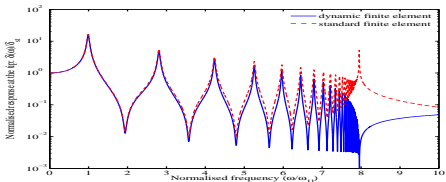
(a) $e_0 a = 0.5 \text{ nm}$



(b) $e_0 a = 1.0 \text{ nm}$



(c) $e_0 a = 1.5 \text{ nm}$



(d) $e_0 a = 2.0 \text{ nm}$

Figure : Amplitude of the normalised dynamic frequency response at the tip for different values of $e_0 a$. Dynamic finite element results (with one element) is compared with the conventional finite element results (with 100 elements).

- Excellent agreement was found for the first 10 natural frequencies.
- However, the results become quite different for the dynamic response.
- In the numerical calculations, 10^5 points are used in the frequency axis. The frequency response functions from the standard finite element were obtained using the classical modal series method [38].
- For small values of $e_0 a$ the results from the dynamic finite element and standard finite element method agree well, as seen in (a) and (b).
- The discrepancies between the methods increase for higher values of $e_0 a$ as seen in (c) and (d).

- The results from the dynamic finite element approach are exact as it does not suffer from error arising due to finite element discretisation.
- For higher values of $e_0 a$, increasing numbers of natural frequencies lie within a given frequency range. As a result a very fine mesh is necessary to capture the high number of modes.
- If the given frequency is close to the maximum cutoff frequency, then a very high number of finite elements will be necessary (theoretically infinitely many and there exist an infinite number of frequencies up to the cut off frequency).
- In such a situation effectively the conventional finite element analysis breaks down, as seen in (d) in the range $7 \leq \hat{\omega} < 8$. The proposed dynamic finite element is effective in these situations as it does not suffer from discretisation errors as in the conventional finite element method.

Summary

- Strain rate dependent viscous damping and velocity dependent viscous damping are considered.
- Damped and undamped natural frequencies for general boundary conditions are derived.
- An asymptotic analysis is used to understand the behaviour of the frequencies and their spacings in the high-frequency limit.
- Frequency dependent complex-valued shape functions are used to obtain the dynamic stiffness matrix in closed form.
- The dynamic response in the frequency domain can be obtained by inverting the dynamic stiffness matrix.
- The stiffness and mass matrices of the nonlocal rod were also obtained using the conventional finite element method. In the special case when the nonlocal parameter becomes zero, the expression of the mass matrix reduces to the classical case.
- The proposed method is numerically applied to the axial vibration of a (5,5) carbon nanotube.

- Unlike local rods, nonlocal rods have an upper cut-off natural frequency. Using an asymptotic analysis, it was shown that for an undamped rod, the natural frequency $(\omega_{k_{\max}}) \rightarrow \frac{1}{(e_0 a)} \sqrt{\frac{EA}{m}}$. This maximum frequency does not depend on the boundary conditions or the length of the rod.
- Near to the maximum frequency, the spacing between the natural frequencies becomes very small. This in turn leads to clustering of the resonance peaks near the maximum frequency.
- For the oscillation frequency of damped systems, the upper cut-off frequency is given by $(\omega_{k_{\max}}) \rightarrow \frac{c}{(e_0 a)} \sqrt{1 - \left(\frac{\zeta_1 c}{2e_0 a}\right)^2}$ where $c = \sqrt{EA/m}$ and ζ_1 is the stiffness proportional damping factor arising from the strain rate dependent viscous damping constant. The velocity dependent viscous damping has no effect on the maximum frequency of the damped rod.
- The asymptotic critical damping factor for nonlocal rods is given by $(\zeta_1)_{\text{crit}} = 2e_0 a \sqrt{\frac{m}{EA}}$.

- The natural frequencies and the dynamic response obtained using the conventional finite element approach were compared with the results obtained using the dynamic finite method.
- Good agreement between the two methods was found for small values of the nonlocal parameter.
- For larger values of the nonlocal parameter, the conventional finite element approach is unable to capture the dynamics due to very high modal density near to the maximum frequency.
- In this case the proposed dynamic finite element approach provides a simple and robust alternative.

Further reading

- [1] A. Eringen, On differential-equations of nonlocal elasticity and solutions of screw dislocation and surface waves, *Journal of Applied Physics* 54 (9) (1983) 4703–4710.
- [2] M. Aydogdu, Axial vibration of the nanorods with the nonlocal continuum rod model, *Physica E* 41 (5) (2009) 861–864.
- [3] M. Aydogdu, Axial vibration analysis of nanorods (carbon nanotubes) embedded in an elastic medium using nonlocal elasticity, *Mechanics Research Communications* 43 (34).
- [4] T. Murmu, S. Adhikari, Nonlocal elasticity based vibration of initially pre-stressed coupled nanobeam systems, *European Journal of Mechanics - A/Solids* 34 (1) (2012) 52–62.
- [5] T. Aksencer, M. Aydogdu, Levy type solution method for vibration and buckling of nanoplates using nonlocal elasticity theory, *Physica E-Low-Dimensional Systems & Nanostructures* 43 (954).
- [6] H. Babaei, A. Shahidi, Small-scale effects on the buckling of quadrilateral nanoplates based on nonlocal elasticity theory using the galerkin method, *Archive of Applied Mechanics* 81 (1051).
- [7] C. M. Wang, W. H. Duan, Free vibration of nanorings/arches based on nonlocal elasticity, *Journal of Applied Physics* 104 (1).
- [8] R. Artan, A. Tepe, Nonlocal effects in curved single-walled carbon nanotubes, *Mechanics of Advanced Materials and Structures* 18 (347).
- [9] M. Aydogdu, S. Filiz, Modeling carbon nanotube-based mass sensors using axial vibration and nonlocal elasticity, *Physica E-Low-Dimensional Systems & Nanostructures* 43 (1229).
- [10] R. Ansari, B. Arash, H. Rouhi, Vibration characteristics of embedded multi-layered graphene sheets with different boundary conditions via nonlocal elasticity, *Composite Structures* 93 (2419).
- [11] T. Murmu, S. C. Pradhan, Vibration analysis of nano-single-layered graphene sheets embedded in elastic medium based on nonlocal elasticity theory, *Journal of Applied Physics* 105 (1).
- [12] J. Yang, X. Jia, S. Kitipornchai, Pull-in instability of nano-switches using nonlocal elasticity theory, *Journal of Physics D-Applied Physics* 41 (1).
- [13] H. Heireche, A. Tounsi, H. Benhassaini, A. Benzair, M. Bendahmane, M. Missouri, S. Mokadem, Nonlocal elasticity effect on vibration characteristics of protein microtubules, *Physica E-Low-Dimensional Systems & Nanostructures* 42 (2375).
- [14] S. Filiz, M. Aydogdu, Axial vibration of carbon nanotube heterojunctions using nonlocal elasticity, *Computational Materials Science* 49 (3) (2010) 619–627.
- [15] S. Narendar, S. Gopalakrishnan, Non local scale effects on ultrasonic wave characteristics nanorods, *Physica E-Low-Dimensional Systems & Nanostructures* 42 (5) (2010) 1601–1604.
- [16] T. Murmu, S. Adhikari, Nonlocal effects in the longitudinal vibration of double-nanorod systems, *Physica E: Low-dimensional Systems and Nanostructures* 43 (1) (2010) 415–422.
- [17] S. C. Pradhan, Buckling of single layer graphene sheet based on nonlocal elasticity and higher order shear deformation theory, *Physics Letters A* 373 (45) (2009) 4182–4188.
- [18] P. Malekzadeh, A. R. Setoodeh, A. A. Beni, Small scale effect on the free vibration of orthotropic arbitrary straight-sided quadrilateral nanoplates, *Composite Structures* 93 (7) (2011) 1631–1639.
- [19] R. D. Firouz-Abadi, M. M. Fotouhi, H. Haddadpour, Free vibration analysis of nanocones using a nonlocal continuum model, *Physics Letters A* 375 (41) (2011) 3593–3598.
- [20] A. A. Pisano, A. Sofi, P. Fuschi, Nonlocal integral elasticity: 2d finite element based solutions, *International Journal of Solids and Structures* 46 (21) (2009) 3836–3849.
- [21] J. K. Phadikar, S. C. Pradhan, Variational formulation and finite element analysis for nonlocal elastic nanobeams and nanoplates, *Computational Materials Science* 49 (3) (2010) 492–499.
- [22] J. F. Doyle, *Wave Propagation in Structures*, Springer Verlag, New York, 1989.
- [23] M. Paz, *Structural Dynamics: Theory and Computation*, 2nd Edition, Van Nostrand, Reinhold, 1980.
- [24] J. R. Banerjee, F. W. Williams, Exact bernoulli-euler dynamic stiffness matrix for a range of tapered beams, *International Journal for Numerical Methods in Engineering* 21 (12) (1985) 2289–2302.

- [25] J. R. Banerjee, Coupled bending torsional dynamic stiffness matrix for beam elements, *International Journal for Numerical Methods in Engineering* 28 (6) (1989) 1283–1298.
- [26] J. R. Banerjee, F. W. Williams, Coupled bending-torsional dynamic stiffness matrix for timoshenko beam elements, *Computer and Structures* 42 (3) (1992) 301–310.
- [27] J. R. Banerjee, S. A. Fisher, Coupled bending torsional dynamic stiffness matrix for axially loaded beam elements, *International Journal for Numerical Methods in Engineering* 33 (4) (1992) 739–751.
- [28] N. J. Ferguson, W. D. Pilkey, Literature review of variants of dynamic stiffness method, Part 1: The dynamic element method, *The Shock and Vibration Digest* 25 (2) (1993) 3–12.
- [29] N. J. Ferguson, W. D. Pilkey, Literature review of variants of dynamic stiffness method, Part 2: Frequency-dependent matrix and other, *The Shock and Vibration Digest* 25 (4) (1993) 3–10.
- [30] J. R. Banerjee, F. W. Williams, Free-vibration of composite beams - an exact method using symbolic computation, *Journal of Aircraft* 32 (3) (1995) 636–642.
- [31] C. S. Manohar, S. Adhikari, Dynamic stiffness of randomly parametered beams, *Probabilistic Engineering Mechanics* 13 (1) (1998) 39–51.
- [32] J. R. Banerjee, Dynamic stiffness formulation for structural elements: A general approach, *Computer and Structures* 63 (1) (1997) 101–103.
- [33] S. Adhikari, C. S. Manohar, Transient dynamics of stochastically parametered beams, *ASCE Journal of Engineering Mechanics* 126 (11) (2000) 1131–1140.
- [34] S. Gopalakrishnan, A. Chakraborty, D. R. Mahapatra, *Spectral Finite Element Method*, Springer Verlag, New York, 2007.
- [35] S. M. Hashemi, M. J. Richard, G. Dhatt, A new Dynamic Finite Element (DFE) formulation for lateral free vibrations of Euler-Bernoulli spinning beams using trigonometric shape functions, *Journal of Sound and Vibration* 220 (4) (1999) 601–624.
- [36] S. M. Hashemi, M. J. Richard, Free vibrational analysis of axially loaded bending-torsion coupled beams: a dynamic finite element, *Computer and Structures* 77 (6) (2000) 711–724.
- [37] J. N. Reddy, Nonlocal theories for bending, buckling and vibration of beams, *International Journal of Engineering Science* 45 (2-8) (2007) 288–307.
- [38] L. Meirovitch, *Principles and Techniques of Vibrations*, Prentice-Hall International, Inc., New Jersey, 1997.
- [39] T. Murmu, S. Adhikari, Nonlocal vibration of carbon nanotubes with attached buckyballs at tip, *Mechanics Research Communications* 38 (1) (2011) 62–67.
- [40] M. Petyt, *Introduction to Finite Element Vibration Analysis*, Cambridge University Press, Cambridge, UK, 1998.
- [41] D. Dawe, *Matrix and Finite Element Displacement Analysis of Structures*, Oxford University Press, Oxford, UK, 1984.
- [42] S. Adhikari, Doubly spectral stochastic finite element method (dssfem) for structural dynamics, *ASCE Journal of Aerospace Engineering* 24 (3) (2011) 264–276.